DOI: 10.1002/ejic.200800258

Syntheses, Structures and Reactivities of $[CpTc(CO)_3X]^+$ and $[CpRe(CO)_3X]^+$

Fabio Zobi,[a] Bernhard Spingler,[a] and Roger Alberto*[a]

Dedicated to Prof. Dr. W. A. Herrmann on the occasion of his 60th birthday

Keywords: Rhenium / Technetium / Cyclopentadienyl ligand / Prodrug

We have synthesized the $[Cp^*M^{III}(CO)_3Br]^+$ complexes (M = Re, ^{99}Tc) and studied their basic chemistry in water and in organic solvents in order to understand if these complexes could be synthons for the preparation of new Re- and ^{99}Tc-based cyclopentadienyl cores for (radio)pharmaceutical applications. The $[Cp^*M^{III}(CO)_3Br]Br$ [M = Re (**1**), ^{99}Tc (**1a**)] complexes were obtained in nearly quantitative yield from the reaction of the corresponding $[Cp^*M^{I}(CO)_3]$ with Br_2 in cold toluene. Compounds **1** and **1a** are photo- and thermally unstable and undergo rapid, bromide concentration-dependent redox reactions at room temperature generating the stable $[Cp^*M^{III}(CO)_3Br][(CO)_3M^{I}(\mu\text{-}Br)_3M^{I}(CO)_3]$ [M = Re (**2**), ^{99}Tc (**2a**)] species as main products. Reaction of **1** with $AgSbF_6$ gives rise to the redox-stable complex $[Cp^*Re^{III}(CO)_3Br]SbF_6$ (**3**). In water, **1** and **1a** produces a mixture of *cis*/*trans*-$[Cp^*M^{III}Br_2(CO)_2]$ isomers [M = Re (*cis*/*trans*-**4**), ^{99}Tc (*cis*/*trans*-**4a**)] via CO release. In methanol, **3** reacts with the solvent to generate the methoxycarbonyl complex *trans*-$[Cp^*Re^{III}(CO)_2Br(COOCH_3)]$ (**5**). Compound **5** is stable under basic conditions. In acidic media it is converted into $[Cp^*Re^{I}(CO)_3]$ as the major product. Kinetic studies with ^{13}C labelled formic acid indicate that formic acid, generated from rapid hydrolysis of methyl formate released from **5**, is the reducing agent and the source of CO. Reaction of **1** with 3-fluorobenzyl alcohol (**3-FBA**), chosen as a simple model of fluorouracil, gives the corresponding alkoxycarbonyl complex $[Cp^*Re^{III}(CO)_2Br(COOCH_2\text{–}C_6H_4F)]$ (**7**). Under acidic conditions **7** rapidly releases **3-FBA** to give $[Cp^*Re^{I}(CO)_3]$. Compounds **2**, **2a**, *cis*-**4**, *trans*-**4a** and **5** were structurally characterized.

Introduction

The recent years have experienced an increase in research in medicinal inorganic chemistry mainly due to the advent of metal complexes for replacing or complementing cisplatin in cancer therapy. Ru complexes, in particular those containing the $[Ru(arene)]^{2+}$ moiety or Ru^{III}-imidazole-based compounds are excellent candidates.[1,2] These complexes have in common that one or two of the ligands can, for instance, be replaced by N7 of guanine in DNA.[3,4] We found that the *fac*-$[Re(CO)_3]^+$ core was also capable of coordinating to two guanine bases in *cis* orientation.[5] We have demonstrated that the guanine ligands did assume both, a HH and a HT conformation around the metal centre. The *fac*-$[Re(CO)_3]^+$ moiety displays a similar reactivity pattern with plasmid DNA as, for example, cisplatin, implying a possible interaction with adjacent guanines in DNA.[6]

Intrigued by the structural features of the $[Ru(arene)]^{2+}$ or $[Cp^*Rh]^{2+}$ cores with three coordination sites stably blocked by η^5- or η^6-aromatic ring, we became interested in extending these building blocks for medicinal purposes to Re based moieties in general and $[CpRe]^{2+}$ in particular. The $[Cp^*Re]^{2+}$ moiety is apparently similar to the above-

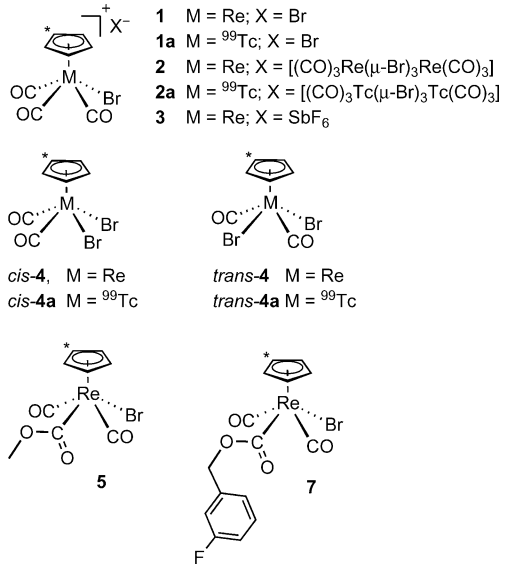

Scheme 1. Summary of Re^{III} and $^{99}Tc^{III}$ complexes.

[a] Institute of Inorganic Chemistry, University of Zürich, Winterthurerstrasse 190, 8057 Zürich, Switzerland
E-mail: ariel@aci.uzh.ch

Supporting information for this article is available on the WWW under http://www.eurjic.org or from the author.

mentioned Ru and Rh cores but its d^4 electronic structure leads to a coordination number of 7. Some synthetic investigations with rhenium exist[7–11] but the chemistry of its technetium homologues is essentially unknown. In particular, the stability and reactivity in water or methanol is crucial in order to assess the versatility of this core for biological purposes. Thus, as the search for novel reactive Re- and Tc-based cores for (radio)pharmaceutical applications is of wide interest, we have studied the chemistry of the $[Cp^*M^{III}(CO)_3Br]^+$ fragment (M = Re, ^{99}Tc) in order to get better insight in the basic reactivity and behaviour of this core in water or methanol. An overview of the newly prepared rhenium and technetium complexes is given in Scheme 1.

Results and Discussion

Synthetic Aspects

Reaction of $[Cp^*M(CO)_3]$ (M = Re, ^{99}Tc) in toluene with Br_2 resulted in the immediate precipitation of yellow $[Cp^*ReBr(CO)_3]Br$ (**1**) or $[Cp^*{}^{99}TcBr(CO)_3]Br$ (**1a**) in almost quantitative yield. This approach is synthetically very convenient since the same reaction in homogeneous solution results in low yield due to the formation of $[(CO)_3M(\mu\text{-}Br)_3M(CO)_3]^-$.[12] Correspondingly, the complexes $[Cp^*MBr(CO)_3][(CO)_3M(\mu\text{-}Br)_3M(CO)_3]$ (for M = Re **2**; for M = ^{99}Tc **2a**) were isolated but not the equivalent Br^- salts (see below). As will become clear later, the formation of the M^I counterion $[(CO)_3M(\mu\text{-}Br)_3M(CO)_3]^-$, which reduces the yield to maximum of 30%, is due to parallel redox processes taking place in solution with **1** and **1a**. It was previously suggested that excess Br_2 might react with the Cp* ligand thereby decreasing the overall yield.[12] We found no difference in the overall yield with excess of Br_2, most likely due to the immediate precipitation of **1** and **1a** from toluene. The halide counterion could be exchanged via ion metathesis with $AgSbF_6$ and the yellow $[Cp^*ReBr(CO)_3][SbF_6]$ (**3**) complex was obtained in good yield from **1**. Further anion exchange can be performed with e.g. $[NO_3]^-$ or $[ClO_4]^-$ but $[SbF_6]^-$ gave the best results.

In the solid state and as isolated from the synthesis, **1a** changes its colour from yellow to blue at room temperature and under N_2 within minutes. Complex **1** is relatively more stable in the solid state and a similar change is observed within a 2 days period only. During this time, the colour of solid or dissolved **1** changes from yellow to orange to dark brown. However, when kept in the dark and at –30 °C, **1** is stable for weeks. Analysis of the solid compounds after a couple of days indicates the formation of an $[M^I(CO)_3]$ species and recrystallization gives $[Cp^*MBr(CO)_3][(CO)_3M(\mu\text{-}Br)_3M(CO)_3]$ (**2**: M = Re; **2a**: M = ^{99}Tc) complex.

In order to confirm the authenticity of the products after solid state decomposition, we examined the CO stretching frequencies by IR spectroscopy of **1** in a KBr matrix over a period of 24 h. The high CO stretching frequency of **1** at 2109 cm^{-1} indicates a reactive carbonyl group making both, thermal and photolytic processes likely decomposition pathways of **1**. Accordingly, **1** was kept in a KBr pellet at room temperature in the dark while another one was placed in a constant stream of cold nitrogen and irradiated by light from a 150-W halogen lamp. The results of these experiments are shown in Figure 1.

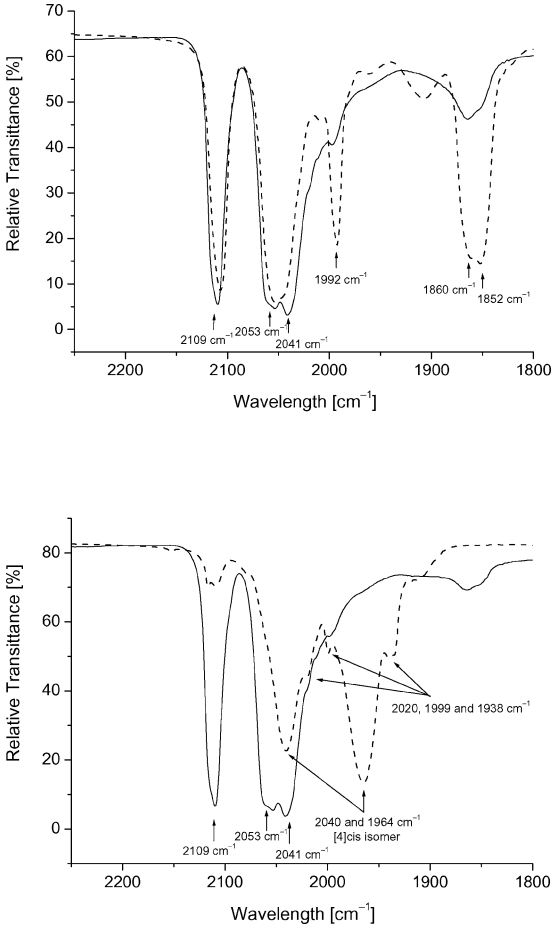

Figure 1. Re–CO IR region (1800–2250 cm^{-1}) showing thermal reactivity in the dark (top) and photo reactivity in the cold (bottom) of **1**. In both cases the solid line indicates the initial spectrum and the dashed line the final spectrum.

The IR spectrum of pure **1** shows three distinct CO stretching frequencies at 2109, 2053 and 2041 cm^{-1}. After 24 h in the dark, three new peaks were observed at 1992, 1860 and 1852 cm^{-1}. The pattern and the position of these new frequencies points to a typical $Re^I(CO)_3$ spectrum of $[(CO)_3Re(\mu\text{-}Br)_3Re(CO)_3]^-$ and are in agreement with those reported for $[NEt_4][(CO)_3Re(\mu\text{-}Br)_3Re(CO)_3]$.[12] It was possible to confirm the authenticity of the complexes formed in the dark at room temperature by X-ray structure analysis. An ORTEP presentation of cations of complexes **2** and **2a** together with relevant bond lengths is given in Figure 2. The structures are discussed in more details later in this text.

If the sample was subjected to light in the cold, the original ν_{CO} bands of **1** disappeared almost completely and the resulting spectrum showed two relatively broad bands at

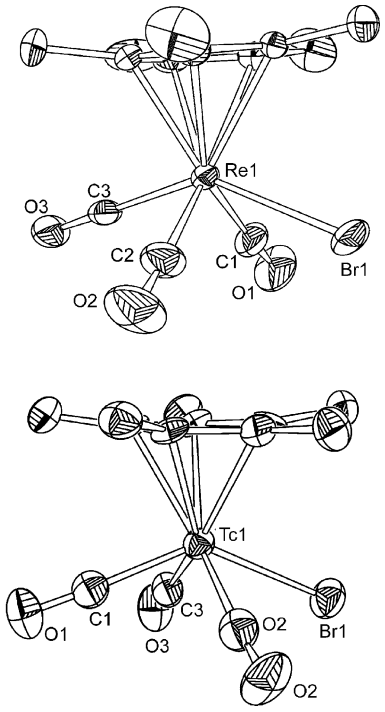

Figure 2. ORTEP presentation of cations of complexes **2** (top) and **2a** (bottom) (50% probability of thermal ellipsoids). Important bond lengths [Å] are: Re1–C1 1.990(5), Re1–C2 1.962(6), Re1–Br1 2.5884(6), C1–O1 1.110(5), C2–O2 1.130(6); ^{99}Tc1–C1 1.974(10), ^{99}Tc1–C2 2.031(11), ^{99}Tc1–C3 2.076(9), ^{99}Tc1–Br1 2.5893(11), C1–O1 1.126(11), C2–O2 1.105(11), C3–O3 1.006(10).

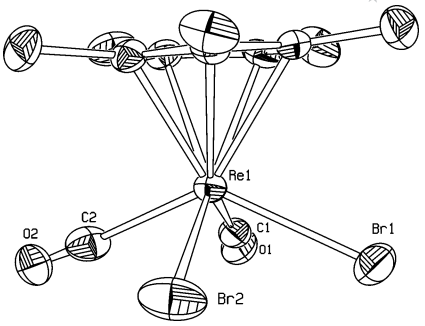

Figure 3. X-ray structure of the cation in *cis*-**4**. Important bond lengths [Å] are: Re1–C1 1.922(13), Re1–C2 1.934(12), Re1–Br1 2.5821(12), Re1–Br2 2.5699(11), C1–O1 1.130(13), C2–O2 1.109(13).

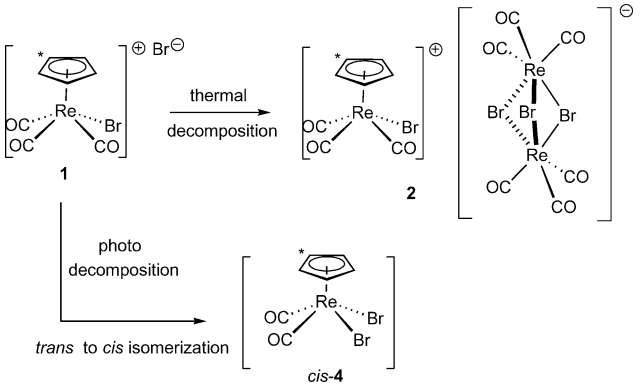

Scheme 2. Solid state reactions of **1**.

2040 and 1964 cm^{-1} with smaller peaks at 2020, 1999 and 1938 cm^{-1}. The former major bands are assigned to the *cis* isomer of [Cp*ReBr$_2$(CO)$_2$] (*cis*-**4**) in agreement with reported values and confirmed by an X-ray structure analysis.[9–11]

Obviously, **1** is thermally unstable, yielding a partially reduced species whereas in the cold under light irradiation, one coordinated CO can easily be cleaved, yielding the very stable complex *cis*-**4**. Mechanistically, release of one CO generates one free coordination site which is occupied by the counterion Br$^-$ resulting in the formation of *cis*-**4** as the major product. Most likely, both the *cis* and *trans* isomer were initially formed and a concurrent solid-state photochemical *trans*→*cis* isomerization took place during irradiation. In fact, it was previously shown that visible light converted *trans*-[CpRe(CO)$_2$X$_2$] (X = Br, I) into the corresponding *cis*-isomer in yields >80%.[13,14] Accordingly, the *trans*-**4** isomer was not observed in this reaction but was isolated as a product from the reaction of **1** in water as discussed below. The reaction with technetium revealed similar spectroscopic features but reactions were substantially faster. It was possible to crystallize *cis*-**4** and to confirm its structure by X-ray analysis. An ORTEP presentation is given in Figure 3. Details about the structures are discussed in the crystallography section. The solid-state reactions are summarized in Scheme 2.

Behaviour in Solution

Complex **1** is not stable in solution and decomposes rapidly to give **2** via redox reactions. The fact that the same complex cation [Cp*Re^{III}(CO)$_3$Br]$^+$ is stable with [SbF$_6$]$^-$ as a counterion implied an inter- and not an intramolecular reaction with the Br$^-$ counterion acting as a reducing agent. To support this mechanism, we examined the rate of reduction of [Cp*Re^{III}(CO)$_3$Br]$^+$ as a function of the Br$^-$ concentration. Given the inherent instability of **1**, the redox stable complex **2** was used as starting material. Addition of excess [Bu$_4$N]Br to a CH_2Cl_2 solution of **2** initiated spectroscopic changes as shown in Figure 4 (see also Supporting Information). The rate of reduction was found to be linearly dependent on [Br$^-$] concentrations. Rate constants k_{obs} are given in Table 1. The assumption of a second-order reaction gave a rate constant of 2.48×10^3 M^{-1} s^{-1}. From the observed rates we conclude that Br$^-$ reduction of **2** is the rate-determining step while loss of the Cp* ligand is fast.

Obviously, compounds **1** and **1a** are strong oxidation agents implying that both compounds are likely to be reduced to lower valent species in blood serum for instance. From a chemical point of view, however, the facile reduction is attractive since it might open a pathway to the very rare class or Re^{II} complexes by one electron reduction.

A further crucial aspect applying the [Cp*M]$^{2+}$ moieties in biology or medicine is the behaviour in water. An interesting feature of the [Cp*Re(CO)$_3$X]$^+$ cation is a high vi-

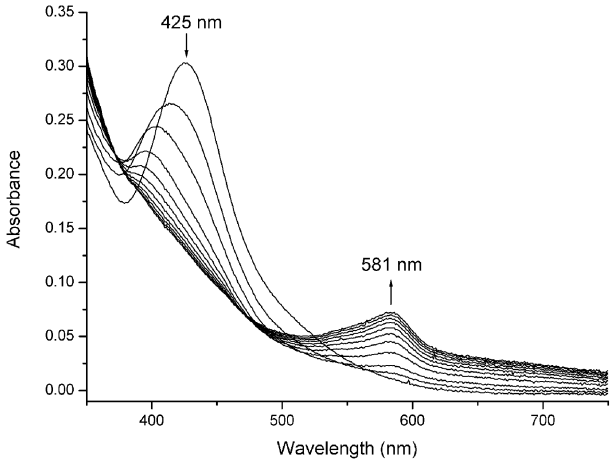

Figure 4. Changes in UV/Vis spectra upon addition of $[Br]^-$ to a solution of **2** in CH_2Cl_2, time intervals are 15 min.

Table 1. $[Bu_4N]Br$ concentration (mM ± 0.01) dependence of the initial rate of reduction (k_{obs}, mM s^{-1}) of **2** (0.1 ± 0.01 mM solution).

$[Bu_4N]Br$	$k_{obsd.}$
0.1	0.030 ± 0.006
0.5	0.102 ± 0.011
1	0.246 ± 0.017
5	1.201 ± 0.036

bration band observed above 2100 cm^{-1}. This weakly bound CO should be prone to substitution by solvent molecules or to attack by nucleophiles. In water, **1** and **1a** are only sparingly soluble but brief sonification of either complex salt results in a yellow suspension consisting of a mixture of *cis* and *trans*-$[Cp^*MBr_2(CO)_2]$ (*cis*/*trans*-**4** for M = Re, *cis*/*trans*-**4a** for M = ^{99}Tc) isomers. The conversion is nearly quantitative with isolated yields typically 45% of *cis*-**4** and 30% of *trans*-**4**. No intermediates such as $[Cp^*ReBr(OH_2)(CO)_2]^+$ could be detected likely due to rapid anion trapping, indicating strong Lewis acidity of the Re^{III} centre. The structure of the complex *trans*-**4a** was confirmed by X-ray structure analysis and an ORTEP presentation is given in Figure 5. Details are discussed in the crystallography part of this article.

The pH of the aqueous solution dropped from about 6 to ca. 2 and the ^1H NMR indicated the formation of small amounts of formic acid. TCD analysis of the head space above the reaction mixture showed the presence of CO but not of H_2. The formation of $[Cp^*M^{III}(CO)_2Br_2]$ therefore occurrs mainly by substitution of CO with bromide as evidenced by the reaction yield. To a minor extent, formation of a metalla-carboxylic acid such as $[Cp^*M^{III}(CO)_2Br(COOH)]$ and subsequent release of formic acid accounts for the observed pH decrease. Diaz et al. suggested a metalla-carboxylic acid for this reaction, liberation of CO_2 and formation of the hydrido complex $[Cp^*Re^{III}BrH(CO)_2]$.[9] Protonation and substitution would then lead to the products. In our reactions and with very sensitive TCD analytics, we observed formic acid but no CO_2 or H_2.

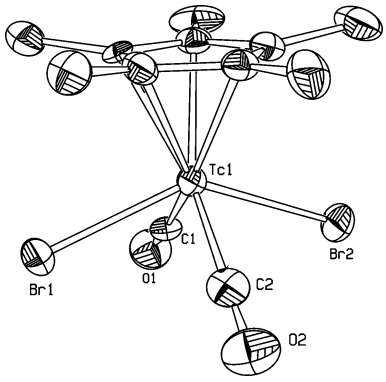

Figure 5. ORTEP of *trans*-**4a** (50% probability of thermal ellipsoids). Important bond lengths [Å] are: ^{99}Tc1–C1 1.982(7), ^{99}Tc1–C2 1.948(8), ^{99}Tc1–Br1 2.5852(8), ^{99}Tc1–Br2 2.5874(7), C1–O1 1.096(7), C2–O2 1.134(7).

In methanol instead of water, complex **3** (redox inactive $[SbF_6]^-$ as a counterion) reacts differently. The high symmetric CO frequency at 2110 cm^{-1} indicates predominant donation from CO to Re which renders the carbon in CO susceptible for nucleophilic attack. Accordingly, **3** reacts rapidly with methanol to form the methyl formate complex *trans*-$[Cp^*Re(CO)_2Br(COOCH_3)]$ (**5**) in 85% yield. The reaction was followed by liquid IR analysis in different solvents and in the presence of methanol. In anhydrous THF or CH_2Cl_2, the IR spectrum of **3** showed ν_{CO} at 2110 and 2044 cm^{-1} respectively (see Supporting Information). Upon addition of CH_3OH to this solution (or in neat CH_3OH), two new bands appear at 2046 and 1976 cm^{-1} while the original bands disappear completely. During the reaction, one proton is released. Addition of bases like imidazole, 1,6-lutidine or NEt_3 results in nearly quantitative formation of **5**. The structure of compound **5** could be confirmed by X-ray structure analysis and a model based on the data is given in Figure 6.

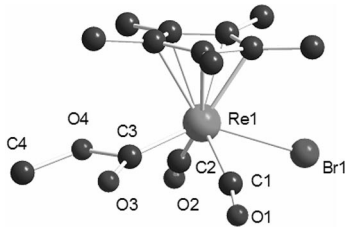

Figure 6. Structural model of **5** based on X-ray data.

The ^1H NMR spectrum ($CDCl_3$) of **5** shows two sharp singlets at δ = 2.00 and 3.64 ppm assigned to the Cp–CH_3 groups and the O–CH_3 protons, respectively. For comparison, ^1H NMR and IR data of the Re and the corresponding ^{99}Tc compounds are summarized in Table 2.

In a 10% D_2O/90% CD_3OD solution pH* > 8, **5** did not show follow-up reactions. Under acidic conditions (pH* < 5), however, an unusual decomposition was observed in that **5** cleanly reacted to $[Cp^*Re^I(CO)_3]$ in about 60% isolated yield. In order to get an insight into this unexpected

Table 2. ^{1}H NMR[a] (δ, ppm) and IR data [cm^{-1}][b] data of Re and ^{99}Tc complexes.

Complex	Cp*[a]	CO *sym.*[b]	CO *asym.*[b]
$[Cp^*Re(CO)_3]$	2.164[c]	2010	1912
$[Cp^*Re(CO)_3Br]^+$ (**2**)	2.286[d]	2110	2050
$[Cp^{*99}Tc(CO)_3Br]^+$ (**2a**)	2.254[d]	–	–
cis-$[Cp^*Re(CO)_2Br_2]$ (*cis*-**4**)	2.055[c]	2052	1971
trans-$[Cp^*Re(CO)_2Br_2]$ (*trans*-**4**)	1.995[c]	2070	1994
cis-$[Cp^{*99}Tc(CO)_2Br_2]$ (*cis*-**4a**)	2.023[c]	2040[f]	1972[f]
trans-$[Cp^{*99}Tc(CO)_2Br_2]$ (*trans*-**4a**)	1.898[c]	2060[f]	1985[f]
$[Cp^*Re(CO)_2Br(COOCH_3)]$ (**5**)	2.002[c]	2046	1974
$[Cp^*Re(CO)_2Br(COOCH_2\text{-}C_6H_4F)]$ (**7**)	1.970[e]	2044	1976

[a] Values referenced to residual solvent peak set at: 7.260 for $CDCl_3$, 1.930 for CD_3CN and 3.300 for CD_3OD. [b] In CH_2Cl_2. [c] In $CDCl_3$. [d] Cations of **2** and **2a** in CD_3CN. [e] In CD_3OD. [f] From ref.[15]

redox reaction, we performed kinetic and NMR studies. The ^{1}H NMR spectrum of **5** in D_2O/CD_3OD 1:9 showed one single Cp–CH_3 signal at 1.995 ppm and the O–CH_3 signal at 3.611 ppm respectively. Addition of trifluoro-acetic acid (TFA), methyl formate or a mixture of both caused disappearance of the original signals and appearance of a new signal at 2.178 ppm, assigned to $[Cp^*Re^I(CO)_3]$. Concomitantly, the resonance of free methanol at 3.336 ppm began to grow. Figure 7 shows the typical change in the ^{1}H NMR spectrum of **5** after addition of trifluoroacetic acid (TFA).

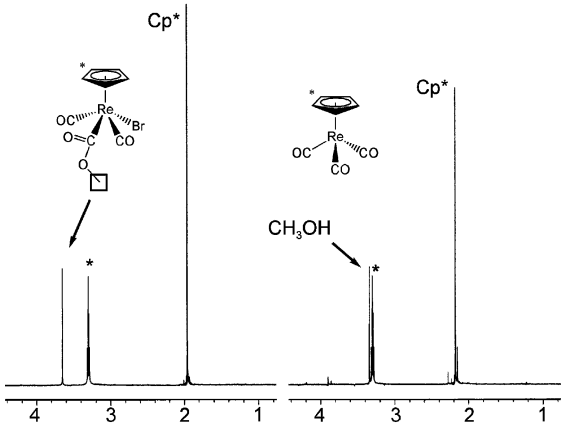

Figure 7. ^{1}H NMR spectrum of **5** (CD_3OD, 0.8–4.4 ppm, left) and the same spectrum after addition of trifluoroacetic acid (TFA) (* indicates residual solvent peak).

Initial observed rate constants of reduction of **5** in the presence of either TFA or methyl formate are similar within experimental error to the rate constant observed in the absence of either reagent (Figure 8 and Table 3). A mixture of both reagents caused a slight but significant increase in the formation of $[Cp^*Re^I(CO)_3]$. When formic acid was added to a solution of **5**, the rate of reduction increased by a factor of about 10.

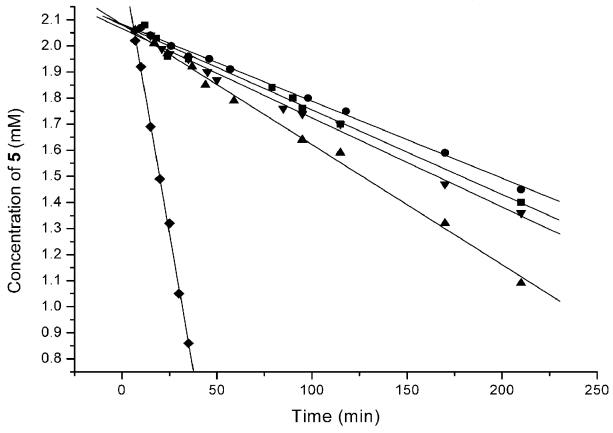

Figure 8. Time-dependent concentration of **5** during its reduction in CD_3OD (●), in the presence of TFA (■), methyl formate (▼), methyl formate plus TFA (▲), formic acid (♦).

Table 3. Initial rate of reduction of **5**[a] to $[Cp^*Re^I(CO)_3]$ (k_{obs}, mM s^{-1}).

Reaction components	$k_{obsd.}$
5	0.198 ± 0.054
5 + TFA[b]	0.180 ± 0.056
5 + methyl formate[b]	0.204 ± 0.048
5 + methyl formate[b] + TFA[b]	0.276 ± 0.061
5 + formic acid[b]	2.502 ± 0.036

[a] 2.47 mM solution. [b] Under pseudo first order conditions.

These data indicate that formic acid causes reduction of **5**→$[Cp^*Re(CO)_3]$ and serves at the same time as a source for CO (Scheme 3). After protonation and cleavage of methyl formate, a reactive intermediate $[Cp^*Re^{III}(CO)_2Br(sol)]^+$ is formed. This intermediate could be generated directly by abstracting a bromide from **4** with $AgSbF_6$ in THF. The $[Cp^*Re^{III}(CO)_2Br(THF)]^+$ cation[16] (**6**) is then allowed to react with excess unlabeled or ^{13}C-labeled formic

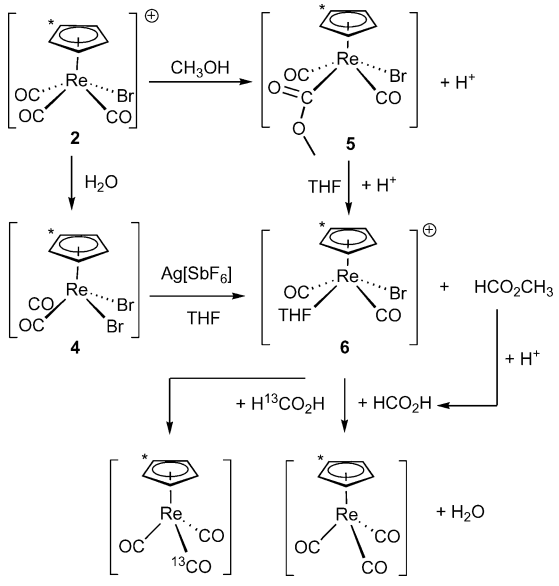

Scheme 3. Summary of reactions leading to reduction of **5** to $[Cp^*Re^I(CO)_3]$.

acid in order to find a proof for our CO source assumption. IR spectra of the reaction with labelled and unlabelled formic acid are shown in Figure 9. In THF, **6** shows two stretching frequencies at 2044 and 1979 cm^{-1}.[16] Reaction with formic acid resulted in two new peaks at 2030 and 1916 cm^{-1} representing $[Cp^*Re^I(CO)_3]$. Performing the same reaction with isotope-enriched $H^{13}CO_2H$ (99% ^{13}C) gave $[Cp^*Re^I(CO)_2(^{13}CO)]$. Correspondingly, the IR frequencies of the product were red shifted by about 30 and 10 cm^{-1}, respectively, for the *symmetric* and *asymmetric* CO stretching modes. A summary of these reactions is given in Scheme 3.

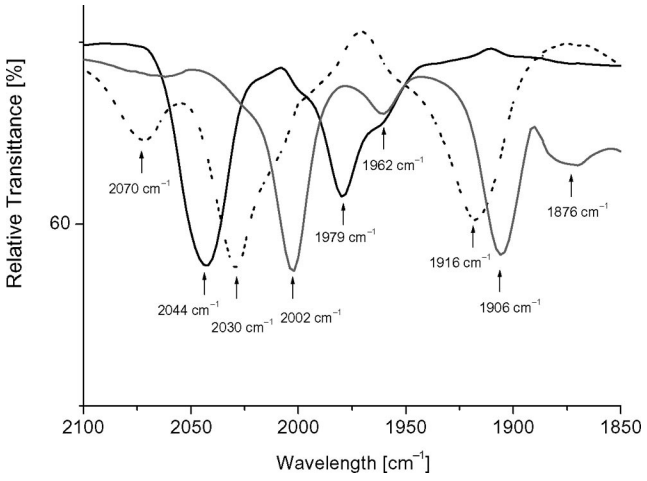

Figure 9. Solution IR spectra (anhydrous THF) of $[Cp^*Re^{III}(CO)_2Br(THF)]SbF_6$ (−), $[Cp^*Re^{III}(CO)_2Br(THF)]SbF_6$ plus HCO_2H (70%THF/30%HCO_2H) (---), $[Cp^*Re^{III}(CO)_2Br(THF)]SbF_6$ plus $H^{13}CO_2H$ (99% ^{13}C, 70%THF/30% $H^{13}CO_2H$) (−).

As often observed, the $[Cp^*Re^I(CO)_3]$ is a thermodynamic sink and is formed as the major product in different reactions involving the {$Cp^{(*)}Re$} moiety. Thermolysis of alkylated acylrhenate and dicarbonylrhenacyclopentane complexes for example gave several organometallic products with $[CpRe(CO)_3]$ being most abundant (ca. 60–70%).[17] Cleavage of $[Cp^*(CO)_2Re(\mu\text{-}CO)Re(CO)(\eta^2\text{-}CH_3C{\equiv}CCH_3)Cp^*]$ or reaction of $[Cp^*(CO)_2Re = Re(CO)_2Cp^*]$ with diethyl fumarate also lead to $[Cp^*Re(CO)_3]$.[18]

X-ray Crystallography

Crystal data and experimental details for the crystallographically characterized complexes **2**, **2a**, *cis*-**4**, and *trans*-**4a** are listed in Table 4 while selected geometrical parameters are listed in Table 5. All compounds occur as discrete molecules in the crystals, with no unusually short inter- or intramolecular contacts. No crystallographically imposed symmetry in the lattice is observed in the structure of **2a**, *cis*-**4** and *trans*-**4a**; however, **2** possess an mirror plane running through O2C2–Re1–Br1 that bisects the Cp* ligand.

Table 5. Selected bond lengths and angles for compounds **2**, **2a**, *cis*-**4**, and *trans*-**4a**.[a]

Compound	**2**	**2a**	*cis*-**4**	*trans*-**4a**
M–C1	1.990(5)	1.974(10)	1.922(13)	1.982(7)
M–C2	1.962(6)	2.031(11)	1.934(12)	1.948(8)
M–C3	1.990(5)[b]	2.076(9)		
M–Br1	2.5884(6)	2.5893(11)	2.5821(12)	2.5852(8)
M–Br2			2.5699(11)	2.5874(7)
C1–M–C2	81.70(16)	81.9(4)	78.7(6)	104.4(2)
C1–M–C3	108.8(3)[b]	79.9(3)		
C2–M–C3	81.70(16)[b]	115.2(4)		
C1–M–Br1	76.26(14)	135.9(3)	77.7(5)	78.21(18)
C2–M–Br1	141.56(15)	75.5(2)	130.2(4)	78.51(19)
C3–M–Br1	76.26(14)[b]	76.4(2)		
C1–M–Br2			127.0(4)	76.13(17)
C2–M–Br2			78.2(4)	76.51(18)
Br1–M–Br2			82.27(5)	138.08(3)

[a] M = transition metal ion (Re for **2** and *cis*-**4**, ^{99}Tc for **2a** and *trans*-**4a**). [b] C3 = C1 by symmetry.

The rhenium and technetium atoms are formally in the +III oxidation state, seven-coordinate and the overall geometry is that of a typical four-legged piano-stool Cp^*ML_4 complex. The M–C(CO) and C–O bonds lengths are in the expected ranges of 1.95–2.15 and 1.10–1.15 Å for metal carbonyl groups.[8,10,17–19] The M–Cp* (centroid) distances range from 1.939(9) for **2a** to 1.960(7) for **2**, and might be viewed as almost identical and evidently insensitive to the differing arrangements of the carbonyl and halide basal ligands in the four structures. Examination of the individual M–C bond lengths to the Cp* ligand reveals, however, systematic differences in structures.

Table 4. Crystallographic data for compounds **2**, **2a**, *cis*-**4**, and *trans*-**4a**.

Compound	**2**	**2a**	*cis*-**4**	*trans*-**4a**
Formula	$C_{19}H_{15}Br_4O_9Re_3$	$C_{19}H_{15}Br_4O_9Tc_3$	$C_{12}H_{15}Br_2O_2Re$	$C_{12}H_{15}Br_2O_2Tc$
FW	1265.55	1000.95	537.26	449.06
T [K]	183(2)	183(2)	183(2)	183(2)
Space group	*Pnma*	$P2_1/c$	$P2_1/n$	$P2_1/c$
Crystal system	orthorhombic	monoclinic	monoclinic	monoclinic
Z	4	4	4	4
a [Å]	17.63762(15)	10.1267(5)	6.8045(5)	8.5009(3)
b [Å]	12.02664(12)	16.2341(13)	26.6199(16)	12.4843(5)
c [Å]	13.26823(13)	17.4224(9)	8.5710(6)	13.7003(5)
β [°]	90	90.178(6)	108.192(8)	102.364(3)
V [Å^3]	2814.47(5)	2864.2(3)	1474.91(17)	1420.26(9)
$d_{calcd.}$ [Mg/m^3]	2.987	2.321	2.420	2.100
R_1 (wR_2)[a]	0.0222 (0.0403)	0.0482 (0.1012)	0.0455 (0.1229)	0.0328 (0.0584)
Largest diff. peak and hole [e Å^{-3}]	1.362 and –2.535	1.095 and –0.672	1.896 and –1.778	0.985 and –0.674

[a] [$I > 2\sigma(I)$].

The individual M–C bonds in the four structures vary, on average, from 2.21(2) to 2.40(2). With reference to the projections in Figure 10, it can be seen that the long M–C bonds are the ones "eclipsed" by the basal ligands with the longest distance observed for the ones "eclipsed" with the halide. The asymmetry follows a pattern typical for $CpML_4$ complexes and can be easily rationalized in terms of the π-acceptor properties possessed by the CO ligands.[20] The CO ligands withdraw π-electron density from the Cp* ring at the expenses of the bonds "pseudotrans" to them. The net effect is a lengthening of the bonds trans to the CO ligands because of the reduced π-contribution of these M–C(Cp) bonds.[20] In **2**, **2a**, *cis*-**4** and *trans*-**4a** there appears to be also a systematic distortion from planarity for the methyl substituents with respect to the average Cp plane. All CH_3 groups are displaced from these planes in a direction away from the rhenium atom with average deviations ranging from 0.05(2) A to 0.26(2) Å. This type of displacement appears to be general in pentamethyl-cyclopentadienyl metal complexes (average deviations ranging from 0.037 to 0.205 Å),[8,10,17–19] with no observable significant statistical variation of the M–C(Cp*) bond lengths.

Complexes **2**, **2a**, *cis*-**4** and *trans*-**4a** also show angular distortion of the four "legs". It is known that when the four L ligands in $CpML_4$ type of complex are not the same, these distort from an ideal pseudo-square-pyramidal geometry in a pairwise fashion.[21] Larger L–M–Ct (where Ct denotes the centroid of the Cp ring) angles are associated with one pair of *trans* ligands. This phenomenon is generally named the "angular trans influence".[22] The distortions in the "legs" can be explained to be largely dependent on the π-bonding ability of the four L ligands with the two metal nonbonding d orbitals. Larger L–M–Ct-angles are associated with stronger π-accepting ligands as a result of a maximization of the π-interaction between the metal d_{z^2} and ligands' π-accepting orbitals. We found that this simple π-model proposed by Poli well applies to our structures.[22] L–M–Ct angles for **2**, **2a**, *cis*-**4** and *trans*-**4a** are given in Table 6 and Figure 11 defines *α* and *α*' angles. In all structures but *cis*-**4** where $\alpha = \alpha'$, *α* (assigned to the *trans*-CO pair) is larger than *α*' (assigned to the other pair of *trans* ligands) well reflecting the greater π-accepting ability of the carbonyl ligand pair.

Table 6. L–M–Ct angles for **2**, **2a**, *cis*-**4** and *trans*-**4a**.

Complex	*α* [°]	*α*′ [°]
2	125–126	108–110
2a	120–124	111–113
cis-**4**	113–118	
trans-**4a**	127–128	110–112

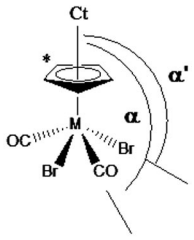

Figure 11. Definition of *α* and *α*′ angles.

The structure of complex **5** was also crystallographically determined. However, residual electron density located below 1 Å above the Cp* ring give a relatively large *R* value.

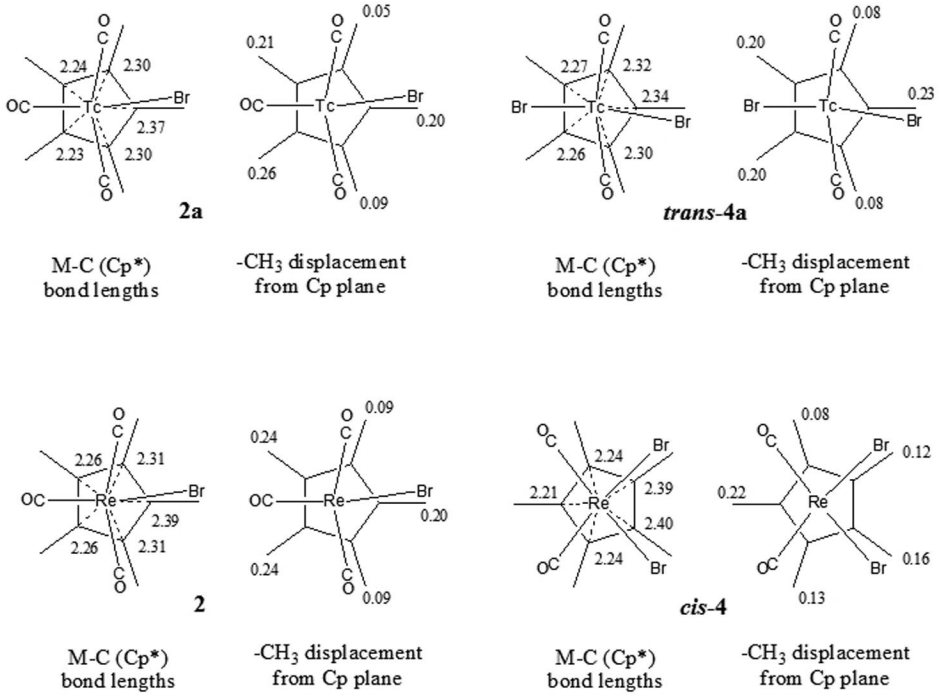

Figure 10. Individual M–C bond lengths of the Cp* ligand and methyl substituents displacement from Cp planes in structures **2**, **2a**, *cis*-**4** and *trans*-**4a**.

For this reason the complex was omitted from our discussion. However, a model of the molecule, derived from X-ray data is given in Figure 6.

Formation Alkoxycarbonyl Complexes as Prodrug Delivery System Models

The redox instability of **1** and **1a** limits the application in biological systems. However, the rapid generation of compounds such as **5** from **3** is intriguing since **3** could be derivatized with other primary alcohols of interest in medicinal chemistry. Thus, $[Cp^*Re^{III}(CO)_3Br]^+$ could provide a scaffold for a prodrug delivery system. The "prodrug" concept/design is a common strategy in medicinal chemistry. Its ultimate objective is to convert an active molecule into a clinically acceptable drug[23] as therapeutically significant molecules may have limited utilization in clinical practice due to poor organoleptic properties, poor aqueous solubility or other adverse effects. A successful examples of this strategy is capecitabine, an orally available prodrug of 5-deoxy-5-fluorouridine, which has recently come into clinical use for the treatment of breast and colorectal cancers.[24] A prodrug approach focused on platinum complexes was also recently suggested by Lippard et al.[25] Comparably, complex **3** (the redox active drug) was treated with 3-fluorobenzyl alcohol (**3-FBA**), chosen as a simple model of fluorouracil. The corresponding (now redox inactive) alkoxycarbonyl complex $[Cp^*Re^{III}(CO)_2Br(COOCH_2\text{-}C_6H_4F)]$ (**7**) (Scheme 4) could be isolated (analytical data of **7** were given in Table 2. See also the Experimental Section).

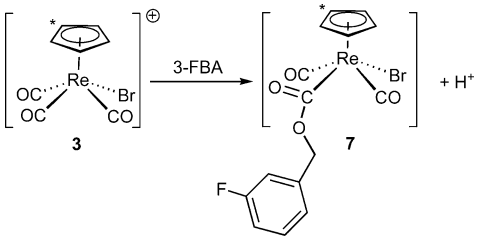

Scheme 4. Formation of $[Cp^*Re^{III}(CO)_2Br(COOCH_2\text{-}C_6H_4F)]$ (**7**).

The prodrug **7** is stable for hours at neutral conditions in water. Under slightly acidic conditions (pH = 6.11), **7** rapidly releases **3-FBA** and converts to $[Cp^*Re^{I}(CO)_3]$. Hydrolysis of the primary alcohol from **7** takes place at significantly higher rate than for example **5**. This opens the possibility to tune the rate of drug activation by selecting the appropriate alcohol.

Conclusions

The complexes $[Cp^*M^{III}(CO)_3Br]^+$ (M = Re, ^{99}Tc) could be synthesized in very good yield. They show different types of reactivities which makes them useful as synthons for $\{Cp^*Re^{III}\}^{2+}$ chemistry. Redox activity and lability of one CO ligand limit the application in medicinal inorganic chemistry at a first glance. However, if redox activity can be "switched on" at a particular site or organ, attractive drugs can be made. As an entry into such a strategy, we showed that reaction of the complexes with primary alcohols produced corresponding carboxy-carbonyl complexes of the type *trans*-$[Cp^*Re^{III}(CO)_2Br(COOR)]$. These complexes are stable under basic or neutral conditions but in slightly acidic media they hydrolyse to $[Cp^*M^{III}(OH_2)(CO)_2Br]^+$ which can then exert its redox activity. Although the $[Cp^*Re^{III}(CO)_3Br]^+$ ion cannot be used for (radio)pharmaceutical applications as formulated, if stabilized, for example, by derivatization at the cyclopentadienyl ring, it could provide a scaffold for a prodrug delivery system.

Experimental Section

Materials: All reagents were used as received. Solvents were distilled prior to use and reactions were carried out under an inert atmosphere. The complex $[Cp^*Re(CO)_3]$ was prepared according to a reported procedures.[26] Infrared spectra were recorded on a Perkin–Elmer BX II spectrometer in KBr pellets or in CH_2Cl_2. All ^{1}H NMR 1D spectra were recorded on a Varian 200 MHz spectrometer; δ values (ppm) were referenced to residual solvent peak set at δ = 7.260 for $CDCl_3$, 1.930 for CD_3CN and 3.300 for CD_3OD.

X-ray Crystallography: All crystals were grown from diffusion of hexane in a CH_2Cl_2 solution of the complex. Suitable crystals were covered with oil (Infineum V8512, formerly known as Paratone N), mounted on top of a glass fibre and immediately transferred to the diffractometer. Crystallographic data for structures **2a** and *cis*-**4** were measured on a Stoe IPDS diffractometer. Data were collected at 183(2) K using graphite-monochromated Mo-K_α radiation (λ = 0.71073 Å). A total of 8000 reflections distributed over the whole limiting sphere were selected by the program SELECT and used for unit cell parameter refinement with the program CELL.[27] Data were corrected for Lorenz and polarization effects as well as for absorption (numerical). Crystals of *cis*-**4** were non-merohedrally twinned. Their X-ray diffraction pattern was integrated with the help of the TWIN program.[27] The tolerance for peak overlap was empirically optimized. The disorder of the Br and CO groups was handled with the appropriate restrains. Crystallographic data for structures **2** and *trans*-**4a** were collected at 183(2) K on an Oxford Diffraction Xcalibur system with a Ruby detector (Mo-K_α radiation, λ = 0.7107 Å) using graphite-monochromated radiation. The program suite CrysAlis^{Pro} was used for data collection, semi-empirical absorption correction and data reduction.[28] All structures were solved with direct method using SHELXS-97[29] or SIR-97[30] and were refined by full-matrix least-squares methods on F^2 with SHELXL-97.[29] The structures were checked for higher symmetry with help of the program Platon.[31] In the structure of *trans*-**4a** a second orientation of the complex was found in the asymmetric unit. Since the occupancy was 4% only the heavy atoms of this minor orientation were localized.

CCDC-680535 (for **2**), -680536 (for **2a**), -680537 (for *cis*-**4**), -680538 (for *trans*-**4a**) contain the supplementary crystallographic data. These data can be obtained free of charge from The Cambridge Crystallographic Data Centre via www.ccdc.cam.ac.uk/data_request/cif.

$[Cp^*Re^{III}(CO)_3Br]Br$ (1): To a stirred solution of $Cp^*Re^{I}(CO)_3$ (120 mg, 0.30 mmol) in toluene (10 mL) at 0 °C, Br_2 (30 µL, 0.59 mmol) was added causing the immediate precipitation of a

bright yellow solid. After 10 min stirring was halted, the product filtered through a fritted funnel and washed with ice cold toluene and ice cold ether. The fritted funnel was wrapped in aluminium foil and the solid dried under vacuum for 1h. The compound was then transferred to a round-bottom flask equipped with a side arm which was evacuated and filled with N_2 three times and then stored at –30 °C. Yield 146 mg, 87%. ^{1}H NMR (200 MHz, CD_3CN): δ = 2.286 (s, 15 H) ppm. IR (solid state): $\tilde{\nu}$ = 2109, 2053, 2041 (C≡O) cm^{-1}. IR (liquid CH_2Cl_2): $\tilde{\nu}$ = 2108, 2057, 2049 (C≡O) cm^{-1}.

[Cp*Tc^{III}(CO)$_3$Br]Br (1a): The same procedure used to synthesize **1** was employed in this case using Cp*Tc^{I}(CO)$_3$ (30 mg scale). Yield 38 mg, 85%. The complex is unstable and decomposes within minutes from its isolation. ^{1}H NMR (200 MHz, CD_3CN): 2.254 (s, 15 H).

[Cp*Re^{III}(CO)$_3$Br]SbF$_6$ (3): To a stirred solution of $AgSbF_6$ (61 mg, 0.18 mmol) in methanol **1** (100 mg, 0.18 mmol) was added causing the immediate precipitation of AgBr. After 5 min stirring was halted, AgBr filtered and the solvent evaporated to dryness. The residue was dissolved in a minimum amount of CH_2Cl_2 and hexane was added resulting in the precipitation of a yellow powder. This product was filtered through a fritted funnel and washed with ice-cold diethyl ether. The fritted funnel was wrapped in aluminium foil and the solid dried under vacuum for 1h. The compound was then transferred to a round-bottom flask equipped with a side arm which was evacuated and filled with N_2 three times and then stored at –30 °C. Yield 50 mg, 39%. $C_{13}H_{15}BrF_6O_3ReSb$ (721.12): calcd. C 21.65, H 2.10; found C 22.88, H 2.51. ^{1}H NMR (200 MHz, CD_3CN): δ = 2.286 ppm (s, 15 H). IR (solid state): $\tilde{\nu}$ = 2109, 2053, 2041 (C≡O) cm^{-1}. IR (liquid CH_2Cl_2): $\tilde{\nu}$ = 2108, 2057, 2049 (C≡O) cm^{-1}.

***cis*/*trans*-[Cp*Re^{III}(CO)$_2$Br$_2$] (*cis*/*trans*-4):** Complex **1** (100 mg, 0.18 mmol) was suspended in water and then sonicated for 30 min at room temp. The resulting brown precipitate containing both isomers of [Cp*Re^{III}(CO)$_2$Br$_2$] was extracted with CH_2Cl_2 and dried with $MgSO_4$. This mixture was chromatographed on a silica gel column prepared in dichloromethane. Successive elution with dichloromethane gave first *trans*-[Cp*Re^{III}(CO)$_2$Br$_2$] (29 mg, 31% yield) from a red band, and finally *cis*-[Cp*Re^{III}(CO)$_2$Br$_2$] (43 mg, 45% yield) from a brown band. Each [Cp*Re^{III}(CO)$_2$Br$_2$] isomer was recrystallized from mixtures of dichloromethane and hexane. $C_{12}H_{15}Br_2O_2Re$ (537.26): calcd. C 26.83, H 2.81; (*cis*) found C 26.91, H 2.74. (*trans*) C 26.41; H 2.39%. ^{1}H NMR (200 MHz, $CDCl_3$): (*cis*) δ = 2.055 (s, 15 H), (*trans*) 1.955 ppm (s, 15 H). IR (solid state): (*cis*) $\tilde{\nu}$ = 2017, 1936 (C≡O), (*trans*) 2042, 1970 (C≡O), 1636 (C=O) cm^{-1}. IR (liquid CH_2Cl_2): (*cis*) $\tilde{\nu}$ = 2033, 1958 (C≡O), (*trans*) (C≡O), 2050, 1981 (C=O) cm^{-1}.

***cis*/*trans*-[Cp*Tc^{III}(CO)$_2$Br$_2$] (*cis*/*trans*-4a):** Complexes *cis*/*trans*-**4a** were obtained as described for *cis*/*trans*-**4**. Yields for *trans*-[Cp*-Tc^{III}(CO)$_2$Br$_2$] and *cis*-[Cp*Tc^{III}(CO)$_2$Br$_2$] were comparable to the Re analogues. ^{1}H NMR (200 MHz, $CDCl_3$): (*cis*) δ = 2.023 (s, 15 H), (*trans*) 1.898 ppm (s, 15 H). IR (liquid CH_2Cl_2): $\tilde{\nu}$ = (*cis*) 2040, 1972 (C≡O); (*trans*) (C≡O), 2060, 1985 (C=O) cm^{-1}.

[Cp*Re^{III}(CO)$_2$Br(CO$_2$CH$_3$)] (5): To a stirred solution of imidazole (30 mg, 0.44 mmol) in methanol (4 mL) at room temperature, **1** (50 mg, 0.09 mmol) was added giving an orange mixture. The reaction was warmed to 37 °C and stirred for 12 h. The solvent was then evaporated under vacuum leaving a light orange solid. A small amount of diethyl ether (2–3 mL) was added resulting in the extraction of complex **5**. Evaporation of the solvent gave **5** as bright orange needles. These were transferred to a round-bottom flask equipped with a side arm which was evacuated and filled with N_2 three times and then stored at –30 °C. Yield 39 mg, 85%. $C_{14}H_{18}BrO_4Re$ (516.40): calcd. C 32.56, H 3.51; found C 32.81, H 3.54. ^{1}H NMR (200 MHz, CD_3OD): δ = 1.994 (s, 15 H), 3.610 ppm (s, 3 H). IR (solid state): $\tilde{\nu}$ = 2029, 1970 (C≡O), 1636 (C=O) cm^{-1}. IR (liquid CH_2Cl_2): $\tilde{\nu}$ = 2045, 1974 (C≡O), 1641 (C=O) cm^{-1}. ESI MS (+ve): *m*/*z* = 539.04 [M] + Na$^+$.

[Cp*Re^{III}(CO)$_2$Br(CO$_2$CH$_2$-C$_6$H$_4$F)] (7): To a stirred solution of imidazole (60 mg, 0.88 mmol) and 3-fluorobenzyl alcohol (**3-FBA**, 114 μL, 1 mmol) in CH_2Cl_2 (8 mL) at room temperature, **1** (100 mg, 0.19 mmol) was added giving an orange mixture. The reaction was warmed to 37 °C and stirred for 12h. The solvent was then evaporated under vacuum leaving an orange oil. A small amount of ether (5–7 mL) was added resulting in the extraction of complex **7**, imidazole and other impurities. The ether fraction was then washed three times with an equal volume of deionized water in order to remove imidazole (final pH of water extract: 8–9) and dried with $MgSO_4$. The solvent was evaporated and the resulting orange oil was dissolved in a minimum amount of a 3% Et_3N in CH_2Cl_2. Silica-gel column chromatography with 3% Et_3N in CH_2Cl_2 as the eluent gave **7** (first eluting orange band) as a viscous orange oil which was transferred to a round-bottom flask equipped with a side arm dried under vacuum then evacuated and filled with N_2 three times and stored at –30 °C. After a while the oil crystallizes at –30 °C. Yield 37 mg, 34%. ^{1}H NMR (200 MHz, CD_3OD): δ = 1.970 (s, 15 H), 5.068 (s, 2 H), 7.021–7.202 (m, 3 H), 7.370 ppm (s, 1 H). IR (liquid CH_2Cl_2): $\tilde{\nu}$ = 2044, 1976 (C≡O), 1655 (C=O) cm^{-1}. ESI MS (+ve): *m*/*z* 633.09 [M] + Na$^+$.

Supporting Information (see also the footnote on the first page of this article): UV/Vis and IR spectra.

[1] a) L. Dadci, H. Elias, U. Frey, A. Hoernig, U. Koelle, A. E. Merbach, H. Paulus, J. S. Schneider, *Inorg. Chem.* **1995**, *34*, 306–315; b) R. E. Morris, R. E. Aird, P. del S. Murdoch, H. Chen, J. Cummings, N. D. Hughes, S. Parsons, A. Parkin, G. Boyd, D. I. Jodrell, P. J. Sadler, *J. Med. Chem.* **2001**, *44*, 3616–3621; c) R. E. Aird, J. Cummings, A. A. Ritchie, M. Muir, R. E. Morris, H. Chen, P. J. Sadler, D. I. Jodrell, *Br. J. Cancer* **2002**, *86*, 1652–1657; d) F. Wang, H. Chen, S. Parsons, I. D. H. Oswald, J. E. Davidson, P. J. Sadler, *Chem. Eur. J.* **2003**, *9*, 5810–5820; e) A. Dorcier, P. J. Dyson, C. Gossens, U. Rothlisberger, R. Scopelliti, I. Tavernelli, *Organometallics* **2005**, *24*, 2114–2123; f) C. A. Vock, C. Scolaro, A. D. Phillips, R. Scopelliti, G. Sava, P. J. Dyson, *J. Med. Chem.* **2006**, *49*, 5552–5561; g) W. H. Ang, E. Daldini, C. Scolaro, R. Scopelliti, L. Juillerat-Jeannerat, P. J. Dyson, *Inorg. Chem.* **2006**, *45*, 9006–9013.

[2] a) B. K. Keppler, W. Rupp, U. M. Juh, H. Enders, R. Niebl, W. Balzer, *Inorg. Chem.* **1987**, *26*, 4366–4370; b) B. K. Keppler, M. R. Berger, M. H. Heim, *Cancer Treatments Rev.* **1990**, *17*, 261–277; c) G. Mestroni, E. Alessio, G. Sava, S. Pacor, M. Coluccia, in *Metal Complexes in Cancer Chemotherapy* (Ed.: B. K. Keppler), VCH, Weinheim, Germany, **1993**, 157; d) G. Sava, I. Capozzi, K. Clerici, R. Gagliardi, E. Alessio, G. Mestroni, *Clin. Exp. Metastasis* **1998**, *16*, 371–379; e) G. Sava, E. Alessio, A. Bergamo, G. Mestroni, *Top. Biol. Inorg. Chem.* **1999**, *1*, 143–169; f) E. Alessio, G. Mestroni, A. Bergamo, G. Sava, in *Metal Ions in Biological Systems* (Eds.: A. Sigel, H. Sigel), Marcel Dekker, New York, **2004**, vol. 42, 323.

[3] a) H. Chen, J. A. Parkinson, S. Parsons, R. A. Coxall, R. O. Gould, P. J. Sadler, *J. Am. Chem. Soc.* **2002**, *124*, 3064–3082; b) H. Chen, J. A. Parkinson, R. E. Morris, P. J. Sadler, *J. Am. Chem. Soc.* **2003**, *125*, 173–186; c) R. Fernández, M. Melchart, A. Habtemariam, S. Parsons, P. J. Sadler, *Chem. Eur. J.* **2004**, *10*, 5173–5179; d) H.-K. Liu, F. Wang, J. A. Parkinson, J. Bella, P. J. Sadler, *Chem. Eur. J.* **2006**, *12*, 6151–6165; e) H.-K. Liu, S. J. Berners-Price, F. Wang, J. A. Parkinson, J. Xu, J. Bella, P. J. Sadler, *Angew. Chem. Int. Ed.* **2006**, *45*, 8153–8156; f) F. Wang, J. Xu, A. Habtemariam, J. Bella, P. J. Sadler, *J. Am.*

Chem. Soc. **2005**, *127*, 17734–17743; g) C. Scolaro, A. Bergamo, L. Brescacin, R. Delfino, M. Cocchietto, G. Laurenczy, T. J. Geldbach, G. Sava, P. J. Dyson, *J. Med. Chem.* **2005**, *48*, 4161–4171; h) C. Scolaro, T. J. Geldbach, S. Rochat, A. Dorcier, C. Gossens, A. Bergamo, M. Cocchietto, I. Tavernelli, G. Sava, U. Rothlisberger, P. J. Dyson, *Organometallics* **2006**, *25*, 756–765.

[4] a) A. D. Kelman, M. J. Clarke, S. D. Edmonds, H. J. Peresie, *J. Clin. Hematol. Oncol.* **1977**, *7*, 274–288; b) M. J. Clarke, in *Metal Complexes in Cancer Chemotherapy* (Ed.: B. K. Keppler), VCH, Weinheim, Germany, **1993**, 129; c) J. M. Brown, A. J. Giaccia, *Cancer Res.* **1998**, *58*, 1408–1416.

[5] F. Zobi, B. Spingler, T. Fox, R. Alberto, *Inorg. Chem.* **2003**, *42*, 2818–2820.

[6] a) F. Zobi, O. Blacque, R. K. O. Sigel, R. Alberto, *Inorg. Chem.* **2007**, *46*, 10458–10460; b) F. Zobi, B. Spingler, R. Alberto, *ChemBioChem* **2005**, *6*, 1397–1405; c) F. Zobi, O. Blacque, H. W. Schmalle, B. Spingler, R. Alberto, *Inorg. Chem.* **2004**, *43*, 2087–2096.

[7] a) R. B. King, *J. Inorg. Nucleic Chem.* **1967**, *29*, 2119–2122; b) A. H. Klahn, C. Manzur, *Polyhedron* **1990**, *9*, 1131–1134.

[8] C. M. Nunn, A. H. Cowley, S. W. Lee, M. G. Richmond, *Inorg. Chem.* **1990**, *29*, 2105–2112.

[9] G. Diaz, A. H. Klahn, C. Manzur, *Polyhedron* **1998**, *7*, 2743–2752.

[10] F. W. B. Einstein, A. H. Klahn-Oliva, D. Sutton, K. G. Tyers, *Organometallics* **1986**, *5*, 53–59.

[11] R. B. King, R. H. Reimann, *Inorg. Chem.* **1976**, *15*, 179–183.

[12] R. Alberto, R. Schibli, A. Egli, U. Abram, S. Abram, T. A. Kaden, P. A. Schubiger, *Polyhedron* **1998**, *7*, 1133–1140.

[13] L. Cheng, N. J. Coville, *Organometallics* **1997**, *16*, 591–596.

[14] L. Cheng, N. J. Coville, *J. Organomet. Chem.* **1998**, *556*, 111–118.

[15] H. H. Knight Castro, A. Meetsma, J. H. Teuben, W. Vaalburg, *J. Organomet. Chem.* **1991**, *410*, 63–71.

[16] F. Godoy, A. H. Klahn, B. Oelckers, *J. Organomet. Chem.* **2002**, *662*, 130–136.

[17] G. K. Yang, R. G. Bergman, *Organometallics* **1985**, *4*, 129–138.

[18] C. P. Casey, R. S. Carino, J. T. Brady, R. K. Hayashi, *J. Organomet. Chem.* **1998**, *569*, 55–60.

[19] a) A. C. Filippou, B. Lungwitz, G. Kociok-Kohn, I. Hinz, *J. Organomet. Chem.* **1996**, *524*, 133–146; b) A. Aballay, E. Clot, O. Eisenstein, M. T. Garland, F. Godoy, A. H. Klahn, J. C. Munoz, B. Oelckers, *New J. Chem.* **2004**, *29*, 226–231; c) J. Bernard, K. Ortner, B. Spingler, H.-J. Pietzsch, R. Alberto, *Inorg. Chem.* **2003**, *42*, 1014–1022; d) A. H. Klahn, B. Oelckers, F. Godoy, M. T. Garland, A. Vegas, R. N. Perutz, C. L. Higgitt, *J. Chem. Soc., Dalton Trans.* **1998**, 3079–3086; e) R. Arancibia, F. Godoy, M. T. Garland, A. Ibanez, R. Baggio, A. H. Klahn, *J. Organomet. Chem.* **2007**, *692*, 963–967; f) T.-F. Wang, C.-C. Hwu, Y.-S. Wen, *J. Organomet. Chem.* **2004**, *689*, 411–418; g) K. I. Goldberg, R. G. Bergman, *J. Am. Chem. Soc.* **1989**, *111*, 1285–1299.

[20] P. Kubacek, R. Hoffmann, Z. Havlas, *Organometallics* **1982**, *1*, 180–188.

[21] Z. Lin, M. B. Hall, *Organometallics* **1993**, *12*, 19–23.

[22] R. Poli, *Organometallics* **1990**, *9*, 1892–1900.

[23] A. Albert, *Nature* **1958**, *182*, 421–423.

[24] a) F. Di Costanzo, A. Sdrobolini, S. Gasperoni, *Crit. Rev. Oncol. Hematol.* **2000**, *35*, 101–108; b) J. L. Marshall, *Oncology* **2001**, *15*, 41–46; c) C. Twelves, M. Boyer, M. Findlay, J. Cassidy, C. Weitzel, C. Barker, B. Osterwalder, C. Jamieson, K. Hieke, *Eur. J. Cancer* **2001**, *37*, 597–604; d) M. L. H. Wang, W. K. A. Yung, M. E. Royce, D. E. Schomer, R. L. Theriault, D. F. Wogan, *Am. J. Clin. Oncol.* **2001**, *24*, 421–424.

[25] D. Wang, S. J. Lippard, *Nature Rev. Drug Discovery* **2005**, *4*, 307–320.

[26] A. T. Patton, C. E. Strouse, C. B. Knobler, J. A. Gladysz, *J. Am. Chem. Soc.* **1983**, *105*, 5804–5811.

[27] *STOE-IPDS Software package*, STOE & Cie, GmbH, Darmstadt, Germany, **1999**.

[28] *CrysAlis^{Pro} Software system*, Oxford Diffraction Ltd., vers. 171.32, Oxford, UK, **2007**.

[29] G. M. Sheldrick, *Acta Crystallogr., Sect. A* **2008**, *64*, 112–122.

[30] A. Altomare, M. C. Burla, M. Camalli, G. L. Cascarano, C. Giacovazzo, A. Guagliardi, A. G. G. Moliterni, G. Polidori, R. Spagna, *J. Appl. Crystallogr.* **1999**, *32*, 115–119.

[31] A. L. Spek, *J. Appl. Crystallogr.* **2003**, *36*, 7–13.

Received: March 11, 2008
Published Online: May 8, 2008

